Journal of Glaciology, Vol. 6, No. 48, 1967

DIELECTRIC RELAXATION IN TEMPERATE GLACIERS

By P. W. F. GRIBBON

(Department of Physics, School of Physical Sciences, University of St. Andrews, Fife, Scotland)

ABSTRACT. The dielectric relaxation of *névé* and glacial ice has been studied on two temperate glaciers in Greenland and France. Measurement of the capacitance and loss tangent in the audio-frequency range of thin parallel wires placed on the surface of a glacier gave ϵ', the relative permittivity, and ϵ'', the loss factor of the *névé*. The relaxation time can be expressed in terms of the frequency f_m at the maximum ϵ'' value of the Cole–Cole $\epsilon''-\epsilon'$ diagram, and its variation with depth was derived from the Cole–Cole diagrams obtained for different wire separations.

For wet 0°C. surface snow in Greenland, $f_m \approx 4$ kHz. and decreased with the increase in density and form factor at greater depths, while for the low-density, cold surface *névé* in France $f_m \approx 2$ kHz. and increased with the increase in temperature at greater depths. All Cole–Cole diagrams showed both impurity-ion losses at low frequencies below 6 kHz., and a spreading factor of the distribution in relaxation times caused by the changes in the physical properties of the glacier with depth. Although the method could not measure temperatures absolutely, relative temperature differences and the position of the 0°C. isotherm were detected when a temperature gradient existed in a glacier.

RÉSUMÉ. *Relaxation diélectrique dans les glaciers tempérés.* La relaxation diélectrique du névé et de la glace de glacier a été étudiée pour deux glaciers tempérés du Groenland et de France. La mesure de la capacitance et de la tangente de perte pour les audio-fréquences de cables fins parallèles placés à la surface d'un glacier donne la permitivité relative ϵ', et le facteur de perte du névé ϵ''. Le temps de relaxation peut s'exprimer en fonction de la fréquence f_m à la valeur maximum ϵ'' du diagramme de Cole–Cole $\epsilon''-\epsilon'$, et sa variation en fonction de la profondeur a été déduite des diagrammes de Cole–Cole obtenus pour différents écartement des cables.

Pour la surface humide à 0°C de neige au Groenland, $f_m \approx 4$ kHz et décroit avec la croissance avec la profondeur de la densité et du facteur de forme, alors que pour la surface d'un névé froid à faible densité en France $f_m \approx 2$ kHz qui croissait avec la croissance de la température avec la profondeur. Tous les Cole–Cole diagrammes montraient à la fois des pertes par impuretés et ions à de basses fréquences inférieures à 6 kHz, et un facteur de dispersion de la distribution des temps de relaxation causée les changements des propriétés physiques du glacier avec la profondeur. Quoique la méthode ne puisse servir à mesurer les températures absolues, les différences de temperature relative et la position de l'isotherme 0°C ont été détectées lorsque dans un glacier existe un gradient de température.

ZUSAMMENFASSUNG. *Dielektrische Relaxation in temperierten Gletschern.* Die dielektrische Relaxation von Firn und Gletschereis wurde an zwei temperierten Gletschern in Grönland und Frankreich untersucht. Die Messung der Kapazitanz und der Verlustspannung im Audiofrequenzbereich dünner paralleler Drähte auf der Gletscheroberfläche lieferte ϵ', die relative Dielektrizitätskonstante, und ϵ'', den Abfallkoeffizienten des Firnes. Die Relaxationszeit kann durch die Frequenz f_m beim Maximalwert für ϵ'' im Cole–Cole-Diagramm für $\epsilon''-\epsilon'$ ausgedrückt werden; ihre Änderung mit der Tiefe wurde aus Cole–Cole-Diagrammen hergeleitet, die für verschiedene Drahtanordnungen aufgestellt wurden.

Für feuchten Oberflächenschnee von 0°C in Grönland war $f_m \approx 4$ kHz und nahm mit dem Anwachsen der Dichte und des Formfaktors in grösserer Tiefe ab. Im lockeren, kalten Oberflächenfirn in Frankreich war $f_m \approx 2$ kHz und nahm mit der Temperatur in grösserer Tiefe zu. Alle Cole–Cole-Diagramme zeigten sowohl Ionenverluste durch Verunreinigungen bei niedrigen Frequenzen unter 6 kHz als auch einen Streuungsfaktor in der Verteilung der Relaxationszeiten, der durch die Änderung der physikalischen Eigenschaften des Gletschers mit der Tiefe hervorgerufen wird. Obwohl die Methode keine absoluten Temperaturen zu messen erlaubte, so lieferte sie doch relative Temperaturen und die Lage der 0°C-Isotherme, wenn im Gletscher ein Temperaturgradient vorhanden war.

1. INTRODUCTION

Recently Evans (1965) has reviewed the dielectric properties of ice and snow. In the review, Robin had suggested that the relaxation of the electric dipoles of ice at audio frequencies might be a basis for the measurement of temperature within large bodies of snow. In 1964 Evans did some preliminary work on the dipole relaxation of snow near Thule in north-west Greenland, and the author used Evans' method to study two temperate glaciers, a highland icefield in West Greenland in 1965, and a plateau snow basin in France in 1966.

This paper covers first (Section 2) the background required to explain the experimental results, outlines the known relaxation spectra of ice and snow, and defines and discusses the measurement of the relaxation time. The experimental procedure (Section 3) gives a brief outline of a theory of the experiment, the equipment used, and the characteristics of the

glaciers being studied. The results are presented in Section 4, and then discussed in terms of the physical properties of a glacier in Section 5.

2. Relaxation Spectra

2.1 *Pure ice*

The relaxation spectrum of pure polycrystalline ice shows that ice is a dielectric solid containing polar molecules that are capable of orientation in an applied A.C. electric field. The motion of the molecular dipoles in the A.C. field is described by an over-critically damped oscillation with a relaxation time τ. Polarization in the ice results in a complex relative permittivity ϵ, which is given by the well-known Debye dispersion relation, Equation (2) in Section 2.3. Ice has several unusual features: for example, the relative permittivity of pure ice at constant temperature can be described by a single relaxation time τ_i, while most solids show a wide distribution of τ; and the long $\tau_i \approx 10^{-4}$ sec. gives a large dispersion in the audio- and low radio-frequency range.

The relaxation time of ice τ_i is influenced by temperature, impurities and stress. The effect of temperature is to produce a thermal agitation of the dipoles which hinders their ordered orientation in the field. When the temperature is lowered, there is an increase in τ_i, since the ability of the dipoles to align in the external field is reduced at low temperatures. τ_i is related to the temperature T through the Boltzmann factor,

$$\tau_i = \tau_0 \exp (W_i/RT) \tag{1}$$

where the characteristic constants of a dipole in ice are the time constant, $\tau_0 = 5{\cdot}3 \times 10^{-6}$ sec., and the activation energy for dipole orientation, $W_i = 13{\cdot}25$ kcal. mole^{-1}, (after Ozawa and Kuroiwa, 1958). A distribution of relaxation times is possible, if the temperature through the ice is not uniform.

Impurities give an increase in the electric conductivity of ice. The presence of cracks, bubbles and other imperfections in ice alter the physical structure of ice and hence its response to an A.C. field. Impurities tend to shorten τ_i (Gränicher and others, 1957; Brill, 1957). Mechanical stress also has been found to shorten τ_i (Westphal, quoted by Evans, 1965).

2.2 *Snow*

The relaxation spectrum of snow is similar to that of ice, but it can show wide variations due to the effect of other factors present in snow. The spectrum is affected by differences in the snow density ρ_s, and structure, as well as by temperature and impurities. Snow changes its internal structure with time, so that not only does ρ_s change but also the arrangement and the linkage between the individual snow crystals. Although the relaxation time of snow τ_s of known density ρ_s is shorter than τ_i of ice (Yosida and others, 1958), there is no obvious way in which τ_s can be related to ρ_s, except to say that τ_s becomes longer with an increase in ρ_s and approaches τ_i. There is no definite relationship between τ_s and temperature T, except that τ_s increases with a decrease in T for a given snow sample. Impurities in snow tend to shorten τ_s. A distribution in τ_s is possible if a temperature or density gradient exists through the snow.

2.3 *Theory and measurement of* τ

A polar dielectric solid, with a complex relative permittivity $\epsilon = \epsilon' - j\epsilon''$, has a frequency dependence given by the Debye dispersion relation,

$$\epsilon = \epsilon_\infty + \frac{\epsilon_0 - \epsilon_\infty}{1 + j\omega\tau}. \tag{2}$$

The relative permittivity ϵ' at a frequency ω is

$$\epsilon' = \epsilon_\infty + \frac{\epsilon_0 - \epsilon_\infty}{1 + \omega^2\tau^2} \tag{3}$$

where ϵ_0 and ϵ_∞ are the relative permittivities in the cases of $\omega \to 0$ and $\omega \to \infty$ respectively.

The loss factor ϵ'' is

$$\epsilon'' = \frac{(\epsilon_0 - \epsilon_\infty)\,\omega\tau}{1+\omega^2\tau^2}. \tag{4}$$

ϵ' is associated with the polarization of charge in the dielectric, and ϵ'' takes account of energy dissipation in the dielectric. The relaxation time τ can be derived from the maximum of the $\epsilon''-\epsilon'$ graph. This follows since all points obeying the Debye relation lie on a semicircle in the $\epsilon''-\epsilon'$ graph. This is a Cole–Cole semicircle, diameter $(\epsilon_0-\epsilon_\infty)$ and centred at $(\epsilon_0+\epsilon_\infty)/2$ on the ϵ' axis: representative Cole–Cole diagrams are shown in Figures 1 and 2. The ϵ'' and ϵ' values measured at different ω form the Cole–Cole semicircle, and the maximum ϵ'' value occurs at an angular frequency ω_m, which satisfies $\omega\tau = 1$ in Equation (4). The maximum frequency, f_m in Hz. or c. sec.$^{-1}$ corresponds to the maximum energy absorption and power loss in the dielectric, and the relaxation time τ is given by

$$\tau = \frac{1}{\omega_m} = \frac{1}{2\pi f_m}. \tag{5}$$

Equation (5) is used to define the relaxation times, τ_i or τ_s, in the present work.

When there is a distribution in τ, the centre of the Cole–Cole semicircle is depressed below the ϵ' axis, and α, the angle expressed in radians, between the ϵ'-axis and the line joining the centre of the circle to ϵ_∞, is the spreading factor of τ (Böttcher, 1952). τ again is defined by Equation (5).

When impurities are present, a Cole–Cole diagram shows high ϵ'' values at low frequencies. This is due to ionic conductivity effects. Impurity ions can give the dielectric an apparent conductivity, $\bar{\sigma}$ in mho m.$^{-1}$, derived from the apparent parallel leakage resistance across the capacitance being observed by the A.C. field. $\bar{\sigma}$ differs from the ohmic conductivity σ and the associated Joule heating losses in a D.C. field, since there are additional power losses, expressible by a loss factor ϵ''', in the A.C. field from dipole reversal in the dielectric. The extra dissipation ϵ''' is related to σ by

$$\sigma = \omega\epsilon_0\,\epsilon''' \tag{6}$$

where ϵ_0 is the relative permittivity in vacuum. Since $\epsilon''' \approx \epsilon''$ at low frequencies ϵ''' can contribute appreciably to the power loss, but at high frequencies $\epsilon''' \ll \epsilon''$ and the effect of ϵ''' is negligible. A Cole–Cole semicircle therefore still can be constructed through the measured ϵ'' and ϵ' values at high frequencies, and τ obtained from the f_m value at the maximum value of ϵ'' of the semicircle.

It has been assumed that impurities, in general, do not affect the dielectric properties of the ice itself with the result that the ϵ_∞, ϵ_0 and f_m values of ice are unaltered by the presence of impurities. This however, is not strictly true (for example see Section 2.1).

There are wide variations possible in the internal structure of ice. Cracks in various directions, air spaces, the orientation of individual crystals, stress, all change the value of ϵ_0 and hence the diameter of the Cole–Cole semicircle with a resultant nett decrease in τ. τ can be obtained also from the relaxation spectrum, or frequency dependence of ϵ' and ϵ''. The spectrum shows that, while ϵ' decreases monotonically with increasing frequency, ϵ'' reaches a maximum at a frequency f_m, given by Equation (5). However, if $\epsilon''' > 0$ at the frequency f_m, the ϵ'' maximum is less definite or even absent, so that τ can not be determined by this method.

2.4 *Cole–Cole diagrams*

Several Cole–Cole diagrams relevant to the present work are shown in Figures 1 and 2.

Figure 1 shows a Cole–Cole diagram of compact snow, $\rho_s = 0{\cdot}4$ g. cm.$^{-3}$, $T = -3{\cdot}0$°C., obtained by Ozawa and Kuroiwa (1958). Curve A is the Cole–Cole semicircle measured immediately after snow was packed into the capacitor used for the ϵ' and ϵ'' measurements,

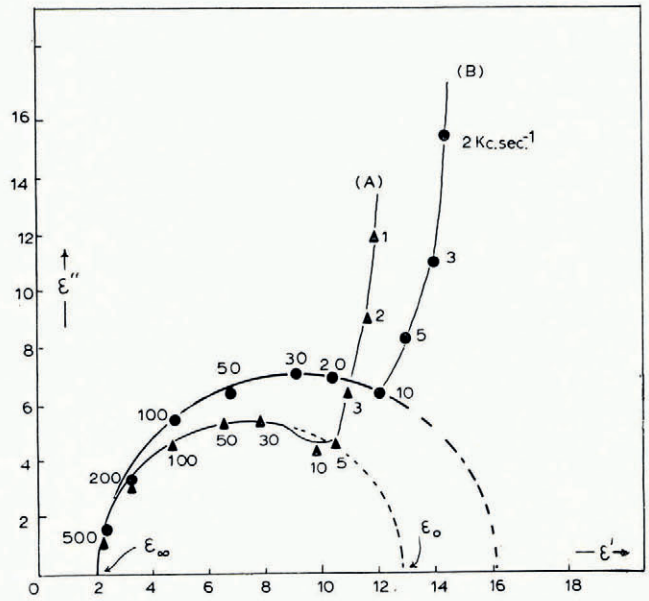

Fig. 1. A Cole–Cole diagram of compact snow of density 0·4 g. cm.⁻³ at −9·0°C. (after Ozawa and Kuriowa, 1958)

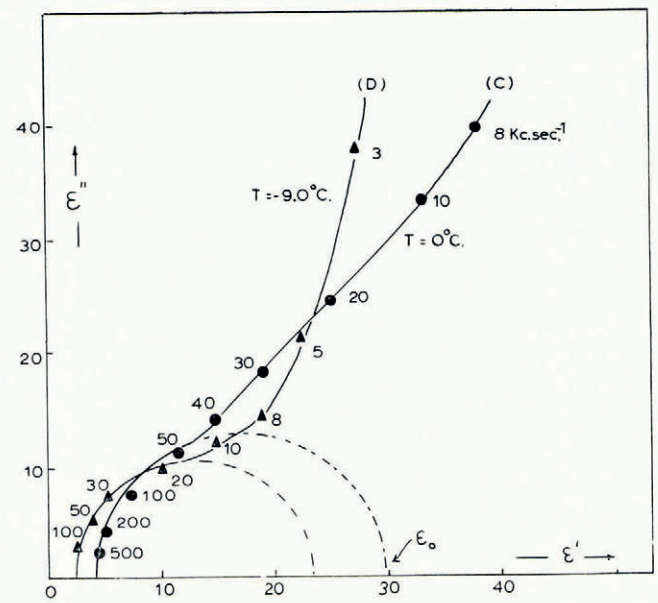

Fig. 2. A Cole–Cole diagram for wet snow of density 0·4 g. cm.⁻³ at 0°C. (Curve C), and for the same snow sample at −9·0°C. (Curve D) (after Ozawa and Kuriowa, 1958)

https://doi.org/10.3189/S0022143000020190 Published online by Cambridge University Press

and curve B is for the same snow after it had been kept at $T = 3{\cdot}0°$C. for 24 hr. ϵ_∞ remained constant, but ϵ_0 increased due to the changes in crystalline structure and the formation of "ice bridges" between the individual snow crystals. Impurity ions were responsible for the rapid rise in ϵ'' at low frequencies. The relaxation time τ_s became longer with time and tended towards τ_i.

Figure 2, curve C, shows the Cole–Cole diagram for wet snow, $\rho_s = 0{\cdot}38$ g. cm.$^{-3}$, $T = 0°$C., that had been studied when the air temperature was $1{\cdot}8°$C. above the freezing point, so that the snow was wet and contained a small percentage of free liquid water. Curve C was obtained after the snow just had been put in the capacitor, and curve D when the snow in the capacitor was placed in a cold chamber maintained at $-9{\cdot}0°$C. In both curves C and D the low frequency, ϵ''' loss contribution was very large. ϵ_∞ and ϵ_0 were decreased by the freezing and the lowering of the snow temperature. It was found also that τ_s for wet snow at 0°C. was less than τ_s for dry compact snow at a temperature just below 0°C.

3. Experimental Procedure

3.1 *Theory of the experiment*

When an A.C. electric field is applied to electrodes placed on top of the surface or within the bulk of a glacier, the electrode system will act as a capacitor with a semi-infinite lossy dielectric between the electrodes. When the electrodes are placed on the surface, the measured values of the capacitance C and the loss tangent D will depend on the dielectric properties of the glacier.

Two wires were placed on the surface, and C and D measured using an A.C. bridge. The electrode system was assumed, following Evans (private communication), to represent a lossy capacitor with an equivalent parallel capacitance C_p given by

$$C_p = \frac{C_s}{1+D^2} \tag{7}$$

where C_s is the series capacitance of the system.
It is assumed to a first approximation also that

$$C_p = G\epsilon' \tag{8}$$

where G is a geometrical factor dependent on the electrode and array dimensions. It follows that

$$\epsilon' = \frac{C_s}{G(1+D^2)}, \tag{9}$$

and, since $D = \epsilon''/\epsilon'$, that

$$\epsilon'' = \frac{DC_s}{G(1+D^2)}. \tag{10}$$

The Cole–Cole diagrams will give f_m or τ.

3.2 *Equipment and its use*

The electrode system was placed on the surface of the glacier. Two thin insulated parallel wires, radius 4×10^{-4} m., were connected at one end to form a Π-shaped array, with maximum wire separation $b \approx 200$ m. and maximum length $l \approx 350$ m. The parallel wires were connected by wires of the same material to an A.C. bridge and oscillator situated half-way between the wires.

An A.C. voltage, $V \approx 1$ or 2 V., was supplied by a Levell transistor *R.C.* oscillator type TG 150 DM, frequency range $1{\cdot}5$ Hz. to 150 kHz., powered by two 9 V. dry batteries. The A.C. bridge was a Marconi TF 2700 transistorized bridge, powered by a 9 V. battery, on which C_s and D could be measured. The bridge usually was easy to balance, although

above 20 kHz., the upper limit for accurate bridge measurements, the null point could be arbitrary. Modifications were made to the A.C. bridge to include an intermediate $D \times 0 \cdot 1$ range between the $D \times 0 \cdot 01$ and $D \times 1$ ranges available on the bridge. All the measured loss tangent values D' had to be scaled by the frequency f, in kHz. at which a measurement was made, to give the correct loss tangent $D = D'f$, since the D values of the bridge were graduated for 1 kHz.

Measurements of C_s and D were made for different frequencies in the range 250 Hz. to 60 kHz. with the first array of small separation, and repeated with different lengths. The wires were held in place at the ends and corners by wood or metal pegs, and additional lengths of wire were added using plastic connectors. The separation then was increased, and the procedure repeated. Correction runs for the capacitance of the side arms were made for large b values.

3.3 *Glaciers under study*

The measurements were carried out on two temperate glaciers; the first being in the Sukkertoppen region of West Greenland, and the second above Chamonix in the French Alps.

The "Big Array" glacier (lat. 65° 45′ 30″ N., long. 52° 18′ W.) lies south of Evighedsfjord in West Greenland and about 50 km. from the open sea. During 1–9 August 1965, the runs were carried out at 855 m., an altitude about 200 m. above the firn line and in the "soaked facies" region of the glacier. Since the air temperature was above freezing point, the upper layers of the glacier consisted of wet snow at 0°C., with a relatively high percentage of free liquid water from summer melt water, and the 7 cm. rain precipitated during 1–4 August. The measured 0°C. snow temperature was in agreement with the estimated snow temperature at a 10 m. depth at the altitude and latitude of the "Big Array" glacier (Mock and Weeks, 1966). The "Big Array" glacier may be classified as "temperate" in its accumulation area, a conclusion in agreement with the "temperate" classification of the Sukkertoppen Iskappe (lat. 66° 15′ N., long. 52° W.), 40 km. to the north, based on temperature measurements made by Bull (1963), Rundle (1965) and Loewe (1966). The lower layers of the glacier in the accumulation area also are assumed to be close to 0°C.

Snow from a pit dug to a depth of 2 m. gave a rather high average $\rho_s = 0 \cdot 77 \pm 0 \cdot 03$ g. cm.$^{-3}$ in the rain-saturated upper snow layer at 0°C. of the "Big Array" glacier. The estimated mean annual snow accumulation was $16 \cdot 5 \pm 1 \cdot 0$ g. cm.$^{-2}$ over the period 1958–64, an accumulation comparable to that of the central area of the Sukkertoppen Iskappe (Bull, 1963).

The glacier at Chamonix was the plateau of the Vallée Blanche at 3550 m., close to the Col de Midi and "Les Cosmiques", the C.N.R.S. laboratory on the Aiguille du Midi. Runs were made in fine weather during 1–4 April 1966. The dry cold upper layers of the glacier were below 0°C. due to the penetration of the winter cold wave into the surface layers of wind-blown consolidated powder snow and underlying *névé*; the air temperature was less than 0°C. Below the region of the cold wave the glacier was at the pressure melting temperature near 0°C. Certain facts are known about the glacier. A *névé* layer, thickness about 30 m., over 150 m. of ice should cover most of the plateau, according to the seismic refraction results of Lliboutry and Vivet (1961). Measurements of the conductivity σ, by Chaillou and Vallon (1964) showed also that in 1963 the plateau was covered by the upper layer of the 1962–63 winter snow accumulation, thickness 7 m. and quite low $\sigma = 10^{-6}$ mho m.$^{-1}$, while just below this layer there was a thin layer of high $\sigma \approx 5 \times 10^{-6}$ to 10^{-5} mho m.$^{-1}$, corresponding to the top surface of the glacier, with its accumulated dust and other impurities formed during the 1962 ablation season. At greater depths the glacial ice had σ fifty times less in the upper layer. It should be noted that a variation of σ with depth may distort an A.C. field penetration and distribution with a corresponding uncertainty in the depth being sampled by the A.C. field.

4. Results

4.1 *Greenland runs*

Twelve useful runs were obtained on the snow of the "Big Array" glacier for six separations b in the range $b = 1 \cdot 8$ m. to 190 m., using different lengths in the range $l = 11$ m. to 365 m. The Π-array was about 0·5 km. from the nearest rock outcrop and centred in a crevasse-free region of the glacier. The array was also moved from the smooth, level snow field to straddle some small surface cracks caused by thin crevasses under the surface, but there was no detectable change in f_m.

The maximum on the $\epsilon''-\epsilon'$ Cole–Cole diagrams was absent in all runs except one. This was due to the additional impurity loss factor ϵ''' present for all frequencies below 6 kHz. A typical run is shown in the Cole–Cole diagram Figure 3. ϵ'' and ϵ' are plotted in arbitrary units, since it is unnecessary here to know the absolute value of the geometrical factor G. The Cole–Cole semicircle for the array, $b = 66 \cdot 3$ m., $l = 110$ m., has $f_m = 5 \cdot 0 \pm 0 \cdot 2$ kHz., and $\alpha = 0 \cdot 64 \pm 0 \cdot 05$ radians. Further discussion of this and other "Big Array" Cole–Cole diagrams is deferred to Section 5.

Three runs were obtained for small b values on wet, bare glacial ice within 50 m. of a rock outcrop at the side of the glacier. A typical Cole–Cole diagram for the glacial ice is shown in Figure 4, in which two Cole–Cole semicircles can be constructed through the measured ϵ' and ϵ'' values. The significance of the two semicircles is discussed in Section 4.2.

4.2 *French runs*

Runs were obtained in the Vallée Blanche for ten separations, in the range $b = 1 \cdot 8$ m. to 170 m., and $l = 8$ m. to 140 m. Twenty runs, series O, were taken with the main arms of the array on the surface of the snow, while ten runs, series I, were taken with the array arms

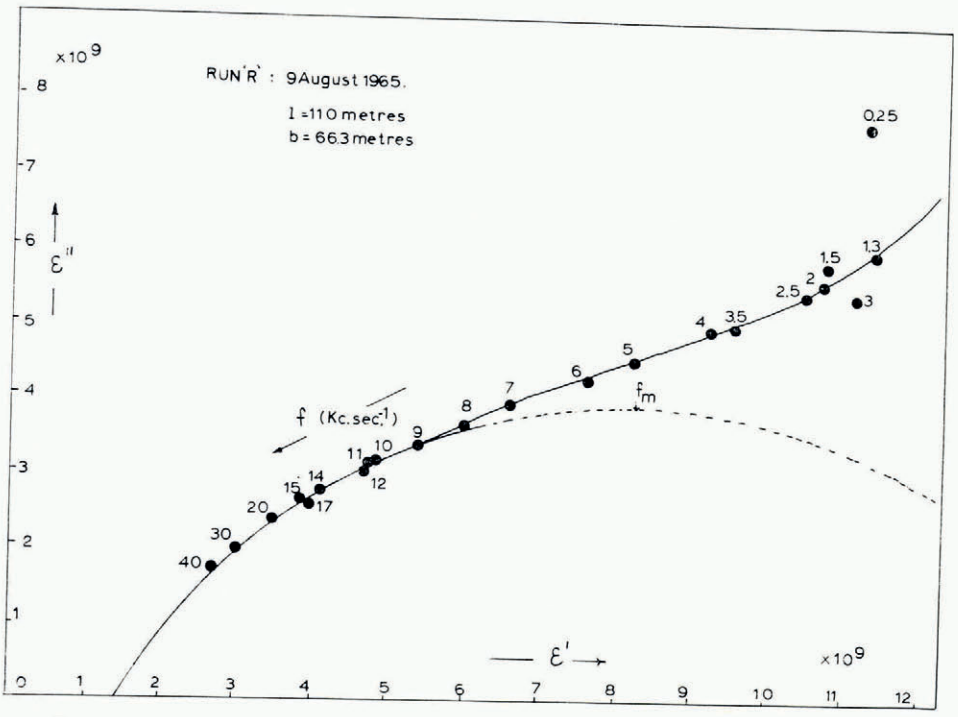

Fig. 3. A Cole–Cole diagram for wet snow, measured on the "Big Array" glacier in West Greenland

https://doi.org/10.3189/S0022143000020190 Published online by Cambridge University Press

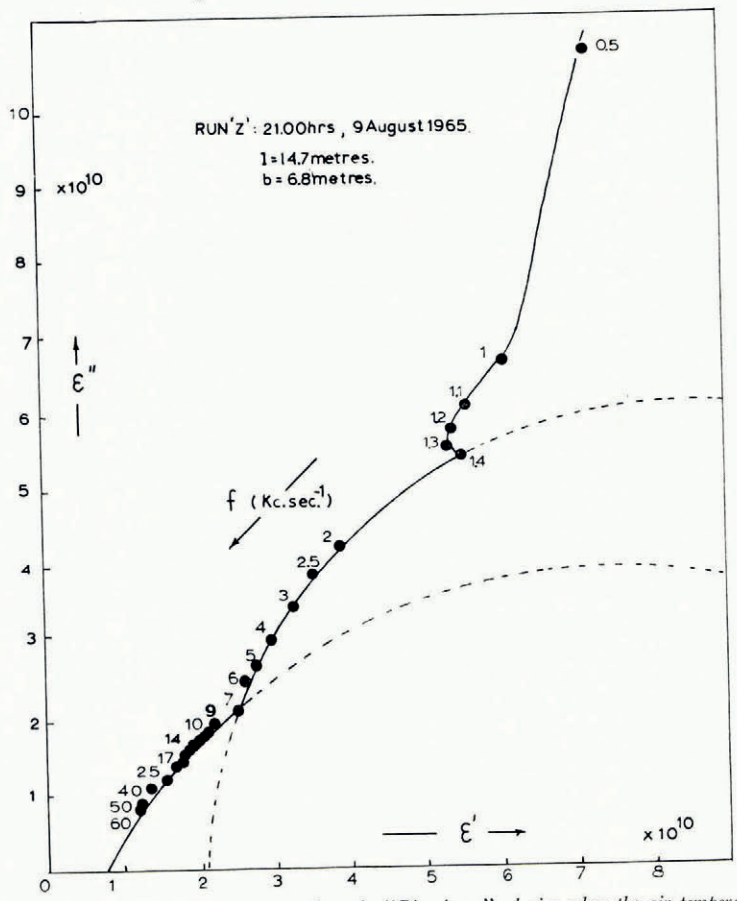

Fig. 4. A Cole–Cole diagram for glacial ice, measured on the "Big Array" glacier when the air temperature was below 0°C.

intentionally buried under a thin snow cover. Readings from run to run were less reproducible than in Section 4.1, while their scatter was greater, particularly at low frequencies and large ϵ'''.

The best series O runs shows two Cole–Cole semicircles. A typical run, with $b = 136$ m. and $l = 91 \cdot 5$ m., is shown in Figure 5. The high-frequency semicircle had $f_m = 2 \cdot 7 \pm 0 \cdot 1$ kHz., and $\alpha = 0 \cdot 58$ radians, and is to be compared with the single Cole–Cole semicircles of the Section 4.1 runs. The lower frequency semicircle, with $f_m \approx 0 \cdot 7 \pm 0 \cdot 1$ kHz., showed no spreading, $\alpha = 0$, and it may represent the response of the snow or ice crystals close to, or frozen on, the surface of the wire electrodes, since it agrees with the response from a homogeneous sample without any spread in τ caused by temperature or density gradients in the sample.

The series I runs also gave two Cole–Cole semicircles and with less scatter in the readings. In general, the series I f_m values were only slightly lower than the series O f_m values, although J. G. Paren (private communication) has shown that C_s and f_m, should depend markedly on the proximity and degree of contact between the snow surface or crystals and the electrode surface.

4.3 *Dependence of f_m and α on b*

The f_m values, obtained from the runs of Sections 4.1 and 4.2, are plotted in Figure 6 as a function of the half-separation $b/2$. It has been considered, by analogy with the equivalent

https://doi.org/10.3189/S0022143000020190 Published online by Cambridge University Press

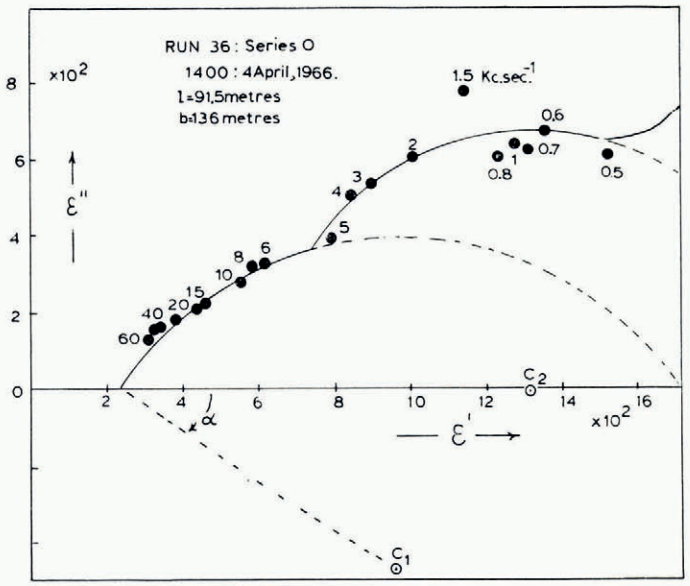

Fig. 5. A Cole–Cole diagram for the névé of the Vallée Blanche, France. C_1 *and* C_2 *are the centres of the two semicircles*

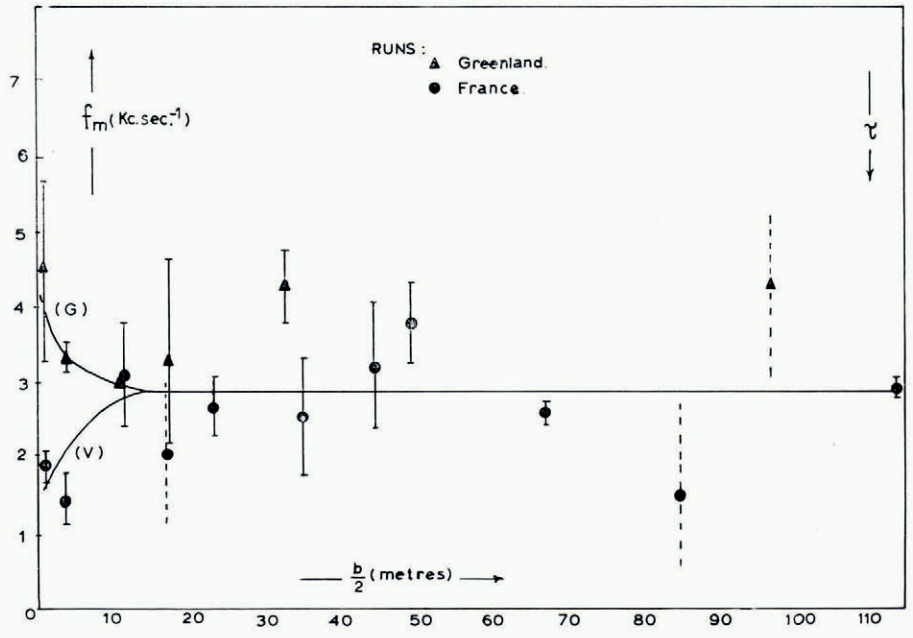

Fig. 6. The variation of the frequency f_m*, at the maximum* ϵ'' *value of the Cole–Cole semicircles, with the half-separation* $b/2$*. The solid-line error bars are the probable errors associated with two or more* f_m *values, the dashed error bars refer to single* f_m *values*

https://doi.org/10.3189/S0022143000020190 Published online by Cambridge University Press

depth used in the determination of earth resistance, etc., that a given f_m value corresponds to a depth $b/2$ equal to one half of the electrode separation distance. Although this assumption may not be justified, it does not invalidate the discussion in Section 5 where the results of Section 4 have been interpreted in terms of the variation with depth of the physical properties of the snow and ice of a glacier. It can be seen that the shape of the f_m graph changed in going from (a) small depths less than about 13 m. where the two sets of results from the Sections 4.1 and 4.2 runs were quite different to (b) greater depths where the two sets were identical within the experimental uncertainty. At small depths $b/2 < \sim 13$ m., the "Big Array" f_m values decreased (Fig. 6, curve G) while the Vallée Blanche f_m values increased (Fig. 6, curve V), while at the greater depths f_m values were constant.

The spreading factor α also varied with depth, as shown in Figure 7. α increased rapidly to a maximum value at a depth of about 3 m. and then decreased to a constant value at depths greater than about 10 m.

5. Discussion

5.1 *Model of a glacier studied by A.C. field*

A cross-section of a glacier is illustrated schematically in Figure 8. A glacier is considered to consist of a series of layers of snow/ice, each layer with its different physical properties having a different relaxation time τ_s. Selected positions of the electrodes (i), (ii), with the associated electric force lines, radii $b/2$, are shown in Figure 8. The force lines were assumed to penetrate uniformly into the layers, and for the lines of radius $b/2$ to divide the total electric flux equally within and without the cylindrical surface defined by the electrode length l and the depth $b/2$. When the wires were in position (i), the relaxation time τ_1 was that of layer 1, but when the wires were in position (ii), the measured τ_s was an average of τ_1 and τ_2 for layers 1 and 2. For the largest depths an average $\bar{\tau}_s$ for all layers was measured. $\bar{\tau}_s$ was not the

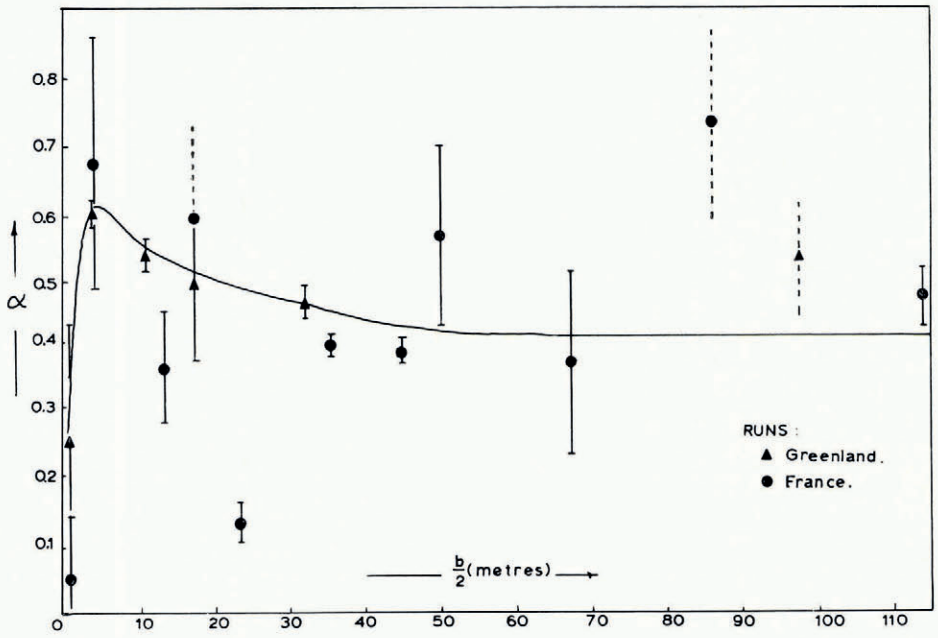

Fig. 7. The variation of the spreading factor α with the half-separation b/2 of the wire electrodes. Error bars are as in Figure 6

https://doi.org/10.3189/S0022143000020190 Published online by Cambridge University Press

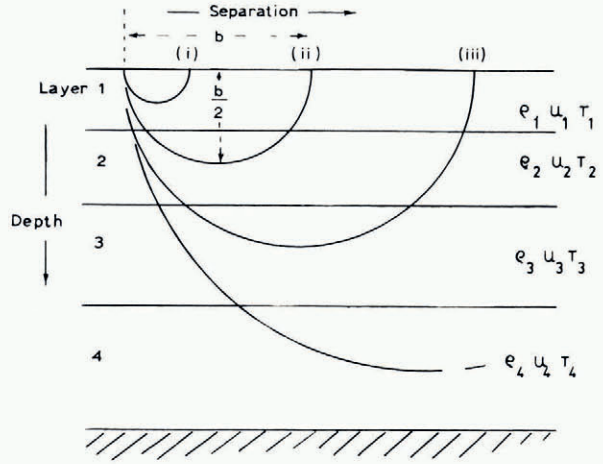

Fig. 8. A hypothetical cross-section of a glacier illustrating the layer structure. The associated densities ρ, Formzahl u, and temperatures T at different depths are indicated. The semicircular field lines associated with the electrode positions (i), (ii), . . . are shown penetrating into layers 1, 2, . . .

arithmetical mean of τ_1, τ_2, etc., because for a distribution in τ_s the resultant Cole–Cole semicircle consisted of the envelope of the individual Cole–Cole semicircles of the layers, in which a slightly different Cole–Cole semicircle resulted from each layer with its different ϵ' and ϵ'' values. This meant that a deeper layer, with its larger ϵ_0 and ϵ'' max. values and hence Cole–Cole semicircle of larger radius, would tend to smear out the smaller semicircles of the shallower layers close to the surface, and the resultant $\bar{\tau}_s$ would be more representative of the deeper layers than of the shallow layers.

5.2 *Significance of Section* 4.3

The important parameters of a layer are its temperature T, its density ρ_s and its form number u. The form number, or *Formzahl*, u expresses the relative proportions of the two components, air and ice, and their arrangement in the snow. τ_s is lengthened by an increase of ρ_s or u, and shortened by an increase in T, so that the τ_s value of a layer at a depth $b/2$ depends on the relative effects of ρ_s, u and T. During the summer ablation periods, a temperate glacier has a constant temperature $T \simeq 0$°C., and any changes in τ_s with an increase in $b/2$ would be due to changes in ρ_s or u. On the other hand, during the winter accumulation period, when a positive temperature gradient exists downward into the glacier, the τ_s value depends on T as well as on ρ_s and u, and the changes in τ_s with $b/2$ would be due to the changes in ρ_s, u, and T. At large depths, all layers would be sampled by the A.C. field, and since T, ρ_s and u have reached constant values there would be no change in f_m or α. This was observed at larger depths, where in Figures 6 and 7 f_m and α were constant for $b/2 > \sim 13$ m.

On the model of a glacier, τ_s at constant temperature should increase, or f_m decrease, with an increase in depth. This was observed, see Figure 6, curve G, where at shallow depths f_m was of the order of 4 kHz., and decreased to $f_m \approx 3$ kHz. at greater depths. The small-depth $f_m \approx 4$ kHz. was an f_m value similar to that of wet glacial ice at 0°C. in the Athabasca Glacier, Columbia Icefield, Canada, measured with parallel plates placed in the surface ice by Watt and Maxwell (1960). At larger depths the present f_m value was lower than the Watt and Maxwell value, $f_m \approx 7$ kHz., obtained with rod electrodes placed in a crevasse at a depth of about 10 m. The difference between the f_m values deep in the glacier may result from the differences either in the physical properties of the snow/ice samples, in the electrode

arrays, or in the effect of ionic conductivity losses. Ionic conductivity losses appeared, on the basis of the Cole–Cole diagrams, (Fig. 3) to be larger in the "Big Array" glacier than in the Athabasca Glacier, which has $\sigma = 5 \times 10^{-7}$ mho m.$^{-1}$. Another difficulty in the interpretation of the f_m values was that the difference between the f_m values for small and large depths was less than the difference to be expected from laboratory measurements (Yosida and others, 1958).

The variation of the spreading factor α at small depths $b/2$ was of interest. It might have been expected, that as $b/2$ increased, there would be an increase in the number of layers sampled until every layer was contributing to the measured ϵ' and ϵ'' values, with the result that α would increase uniformly up to a constant value. Figure 7 shows that the runs, both at "Big Array" and Vallée Blanche, gave a maximum α value at $b/2 \approx 3$ m. This 3 m. depth was small compared to for example the 7 m. depth of Vallée Blanche *névé*. However since α was obtained from the spread of the Cole–Cole semicircles, each corresponding to a different layer with its own ρ_s, u and T, there is no reason why α should not show a maximum value. This can be explained as follows. It is known that the ϵ_0 and ϵ'' maximum values for snow are less than those of ice. At small $b/2$, a certain α was obtained from the envelope of the Cole–Cole semicircles for snow, but at greater $b/2$ these semicircles became swamped by the larger Cole–Cole semicircles of the higher ρ_s and u, consolidated snow of the lower layers of the glacier. An α value based on the larger semicircles would be smaller than one based on the intermediate situation where both small and large semicircles contributed to the measured α value, and a maximum α value would occur in the intermediate region. The relative importance of the small and large semicircles from different depths could not be determined directly, since the ϵ' and ϵ'' values were arbitrary rather than absolute values.

It is also possible to propose an explanation of the low f_m, or long τ_s, values at small depths in the Vallée Blanche (Fig. 6, curve v). This result implied that the present method can detect temperature differences in a glacier, since τ_s, associated with the low temperature of the cold, dry Vallée Blanche *névé*, was longer than either τ_s of the deeper region of the Vallée Blanche glacier or τ of the wet, 0°C. "Big Array" snow. However, there was a fundamental difficulty in relating f_m to the correct temperature, since the temperature dependence of f_m is not known. Nevertheless, an estimate of the upper limit of temperature in the Vallée Blanche *névé* can be made, if three assumptions are used: (a) that at 0°C. $f_m \approx 3$ kHz., (b) that f_m for snow has the logarithmic temperature dependence of Equation (1), and (c) that the activation energy of *névé*, W_n, is less than W_i of ice. The estimated temperature then is less than −5·0°C.: the correct temperature would have been in the range −15°C. to −25°C.

The depth of the 0°C. isotherm was about 13 m. down in the Vallée Blanche *névé* at the time of the series O runs. This followed from the constant value $f_m \approx 3$ kHz. for snow at 0°C. at depths greater than about 13 m. A 13 m. depth was in agreement with a measured position of the 0°C. isotherm at about 15 m. just before the start of the summer ablation period (Lliboutry, 1965).

The constant f_m value at the largest depths ~120 m. indicated that the bedrock had not affected the f_m value. No effect was expected for the Vallée Blanche where the bedrock was about 180 m. below the surface of the snow. The constancy of the f_m values on the "Big Array" glacier indicated that its depth was greater than about 100 m. Further work is planned to use the method for the determination of the depth of snow and ice bodies.

In summary, the dielectric relaxation measurements have indicated that

(i) temperature differences due to the penetration of a winter cold wave into *névé* can be detected,

(ii) the 0°C. isotherm in a temperate glacier can be located,

(iii) a detailed theory of the dielectric properties in a glacier is lacking.

6. Acknowledgements

The work was initiated by a suggestion made by Dr. G. de Q. Robin and Dr. S. Evans of the Scott Polar Research Institute, Cambridge. Acknowledgements are given also for technical assistance provided by D. M. McCall, and H. Cairns of the School of Physical Sciences, University of St. Andrews.

The realization of the "Big Array" experiment was possible from the efforts made by the members of the University of St. Andrews West Greenland Expedition 1965, in particular to C. S. M. Doake for much discussion and assistance in all aspects of the work, to J. C. S. Gilchrist for help with the equipment and in processing the data for the I.B.M. 1620 computer, and to R. W. Hilditch for assistance in the field. The expedition gratefully acknowledges the financial help provided from many sources, and specifically the travel grants (C.S.M.D. and J.C.S.G.) from the Sir James Caird Travelling Scholarship Trust for the "Big Array" work.

The author also acknowledges the co-operation and assistance given by Professor L. Lliboutry and members of the Laboratoire de Glaciologie et Géophysique of the University of Grenoble, and for the use of the facilities and the technical help given at the C.N.R.S. laboratoires at Chamonix and the Col du Midi.

MS. received 20 December 1966

REFERENCES

Böttcher, C. J. F. 1952. *Theory of electric polarisation*. Amsterdam, Elsevier Publishing Co.

Brill, R. 1957. Structure of ice. *U.S. Snow, Ice and Permafrost Research Establishment. Report* 33.

Bull, C. 1963. Glaciological reconnaissance of the Sukkertoppen ice cap, south-west Greenland. *Journal of Glaciology*, Vol. 4, No. 36, p. 813–16.

Chaillou, A., *and* Vallon, M. 1964. Étude de la zone corticale des glaciers tempérés par prospection électrique, avec un potentiomètre d'impédance d'entrée infinie. *Annales de Géophysique*, Vol. 20, No. 2, p. 201–05.

Evans, S. 1965. Dielectric properties of ice and snow—a review. *Journal of Glaciology*, Vol. 5, No. 42, p. 773–92.

Gränicher, H., *and others*. 1957. Dielectric relaxation and the electrical conductivity of ice crystals, by H. Gränicher, C. Jaccard, P. Scherrer and A. Steinemann. *Discussions of the Faraday Society*, No. 23, p. 50–62.

Lliboutry, L. 1965. *Traité de glaciologie. Tom. 2*. Paris, Masson et Cie.

Lliboutry, L., *and* Vivet, R. 1961. Épaisseurs de glace et débit solide de la Vallée Blanche supérieure (Massif du Mont-Blanc). *Comptes Rendus Hebdomadaires des Séances de l'Académie des Sciences* (Paris), Tom. 252, No. 15, p. 2274–76.

Loewe, F. 1966. The temperature of the Sukkertoppen ice cap. *Journal of Glaciology*, Vol. 6, No. 43, p. 179. [Letter.]

Mock, S. J., *and* Weeks, W. F. 1966. The distribution of 10 meter snow temperatures on the Greenland Ice Sheet. *Journal of Glaciology*, Vol. 6, No. 43, p. 23–41.

Ozawa, Y., *and* Kuroiwa, D. 1958. Dielectric properties of ice, snow and supercooled water. *Monograph Series of the Research Institute of Applied Electricity, Hokkaido University*, No. 6, p. 31–37.

Rundle, A. S. 1965. Glaciological investigations on Sukkertoppen ice cap, southwest Greenland, summer 1964. *Ohio State University. Institute of Polar Studies. Report* No. 14.

Watt, A. D., *and* Maxwell, E. L. 1960. Measured electrical properties of snow and glacial ice. *Journal of Research of the National Bureau of Standards* (Washington, D.C.), Sect. D, Vol. 64, No. 4, p. 357–63.

Yosida, Z., *and others*. 1958. Physical studies on deposited snow. V. Dielectric properties, by Z. Yosida, H. Oura, D. Kuroiwa, T. Huzioka, K. Kojima and S. Kinosita. *Contributions from the Institute of Low Temperature Science* Ser. A, No. 14, p. 1–33.